

The Partial Equilibrium Diagram of the Fe-Ge System in the Range 40-72 at. % Ge, and the Crystallisation of some Iron Germanides by Chemical Transport Reactions

MARCUS RICHARDSON

Institute of Chemistry, University of Uppsala, Uppsala, Sweden

Phase relationships in the 40–72 at. % region of the Fe-Ge system have been studied and are incorporated in a revised phase diagram of the system. A low-temperature polymorph of FeGe with the B20 structure ($a = 4.700 \text{ \AA}$) has been found. At about 630°C, this phase transforms to the B35 modification ($a = 5.0029 \text{ \AA}$, $c = 4.0551 \text{ \AA}$), which in turn transforms at 740°C to a new FeGe polymorph with the monoclinic CoGe structure-type ($a = 11.838 \text{ \AA}$, $b = 3.9371 \text{ \AA}$, $c = 4.9336 \text{ \AA}$, $\beta = 103.514^\circ$). The monoclinic polymorph decomposes peritectoidally to $\eta + \text{FeGe}_2$ at 750°C. The κ phase has been found to become homogeneous at 45.5 at. % Ge, and to decompose peritectoidally at 740°C to $\eta + \text{B35 FeGe}$, or (alternatively) $\eta + \text{monoclinic FeGe}$. $\text{Sin}^2\theta$ values are listed for the κ phase. Methods are described for the preparation and crystallisation of single phases by chemical transport with bromine and iodine.

Recent interest in the magnetic structures of iron germanides has led to a more detailed knowledge of the phase relationships in this system. Between 33–67 at. % Ge there is now known to occur seven phases, including the two new polymorphs of FeGe reported in this and a previous paper.¹ The β -phase, or $\text{Fe}_{(2-x)}\text{Ge}$, is ferromagnetic, and was first reported by Ruttewit and Masing² in a metallographic study of the Fe-Ge system. Castelliz³ reported the structure to be of the partially-filled NiAs type ($B8_2$). A recent single-crystal X-ray study of $\text{Fe}_{1.67}\text{Ge}$ by Forsyth and Brown⁴ has shown that the structure is a distorted form of the $B8_2$ type, and that the true space group is $P\bar{3}m1$. Crystals show a spurious $6/mmm$ Laue symmetry through random twinning on (110). Kanematsu⁶ has investigated the β and η phases by magnetic and X-ray methods, and proposes a partial phase diagram on the basis of these results. A structure for the η phase has been proposed by Kanematsu *et al.*⁵ The η phase has hexagonal symmetry, and is related to the β phase by a doubling of the a axis. Powder diffraction lines from a new phase, κ , with composition 43.5 at. % Ge were observed by Kanematsu,⁶ and also by Olofsson.⁷ An iron

monogermanide with the B35 (CoSn-type) structure was reported by Ohoyama *et al.*⁸ and by Shtol'ts and Gel'd.⁹ Single-crystal structural refinements of the two new iron monogermanide polymorphs with the CoGe- and B20-type structures have been reported by the author in an earlier paper.¹ The phase diagram of Ruttewit and Masing² indicates a considerable range of homogeneity for the FeGe₂ phase. The structure was determined to be C16 (CuAl₂-type) by Wallbaum¹⁰ and found to be homogeneous at 66.7 at.% Ge with a negligible range of homogeneity by Shtol'ts and Gel'd.¹¹ The present investigation of crystal structures and phase relationships in the region of 50 at.% Ge was begun when it was found that chemical transport experiments produced some new phases that had not been reported in the literature.

EXPERIMENTAL

Preparation of alloys. Alloys were prepared by melting together lumps of spectroscopically-standardised iron rod (Johnson, Matthey & Co., Ltd: impurities in ppm: C 300, O 100, N 100, Mn 4, Si 2, Ni 2, Cu and Mg both <1) and chips from a germanium ingot (Koch Light Laboratories Ltd., claimed purity 99.999 %). Details of four alloying experiments are given in Table 1, which also shows the loss of germanium occurring in each case.

Heat treatment of alloys. After homogenising treatment, ingots were broken into lumps and sealed into evacuated silica capsules. Heating was carried out for periods of about one week for temperatures above 750°C, and ten days or more at lower temperatures. Capsules were rapidly cooled in water.

Phase analysis and determination of cell dimensions. Powder diffraction photographs were recorded in Guinier-Hägg focussing cameras using either strictly-monochromatic

Table 1. Preparation and homogenisation of Fe-Ge alloys.

	Atomic percent Ge	Alloying and homogenisation treatment	Ge loss at. %
1.	42	Melted in arc furnace under 1 atm. Ar. Repeated three times with turning of specimen between meltings. Homogenised 3 days at 850°C in evacuated silica capsule.	1.7
2.	50	Melted under 1/2 atm. Ar in Al ₂ O ₃ crucible in high-frequency furnace with Ta susceptor. (30 min at 1300°C) Homogenised 10 h at 720°C <i>in vacuo</i> (10 ⁻⁵ torr).	0.06
3.	50	Melted 7 days at 1000°C in Al ₂ O ₃ crucible sealed in evacuated silica capsule. Homogenised 7 days at 700°C.	<0.01
4.	52	Melted in Al ₂ O ₃ crucible for 30 min at 1050°C <i>in vacuo</i> (10 ⁻⁵ torr) in high-frequency furnace with Ta susceptor. Homogenised as in 2.	1.2

CrK α_1 radiation ($\lambda = 2.28962 \text{ \AA}$) or CuK α_1 radiation ($\lambda = 1.54051 \text{ \AA}$) with an aluminium filter to reduce fluorescence radiation from the specimen. Silicon was added as internal reference standard ($a = 5.43054 \text{ \AA}$), and the temperature was $20 \pm 2^\circ\text{C}$ during the exposures. Cell dimensions were refined by a least-squares computer program except in the case of the two cubic phases. Standard deviations are those calculated by the program, and do not include any estimate of systematic errors.

The temperature of the eutectic reaction isotherm between η and FeGe $_2$ was established by differential thermal analysis. A sample of B20 FeGe prepared by chemical transport (see the following) was used to determine the temperature of the polymorphic transformation to B35 FeGe. Powder patterns were taken after heating for several hours at each temperature in a series of increasing temperatures.

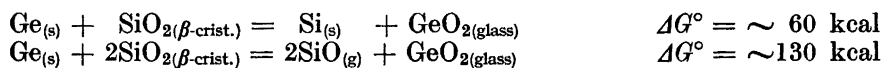
Chemical transport and mineralisation. Silica capsules were charged with about 1 g of alloy ("feedstock"), and a small quantity of bromine or iodine introduced after evacuation and before sealing the tubes. Iodine was either added directly as solid before pumping and sealing, or sublimed into the capsule from a capillary that could be broken after the system had been evacuated. Bromine was introduced in the elemental form in a similar way from sealed capillaries, or alternatively anhydrous FeBr $_2$ was added directly before evacuation and sealing. Capsules were evacuated to a pressure of about 10^{-2} torr, and were not degassed. In the mineralisation experiments the maximum temperature difference between various parts of the capsule was 1°C , and for transport a difference of from 3 to 73°C was applied, with the feedstock at the hotter part of the tube.

Details of a number of transport and mineralisation experiments are summarised in Table 2.

DISCUSSION OF PREPARATIONS

Several Fe-Ge alloys were made by sintering spectroscopically-standardised iron powder with powdered semiconductor-grade germanium. There were indications of a loss of germanium from such specimens, and the same observation was made for alloys prepared according to the methods of Table 1 and subsequently ground to powder, pressed to pastilles, and heated in evacuated capsules. Furthermore, a non-metallic product was usually seen on the surface of sintered pastilles, suggesting that some oxidation had occurred. This is not surprising in view of the fact that iron and germanium powders can contain up to at least 5 wt% oxygen unless specially prepared. Jolly *et al.*¹² found ~ 3 wt% O in a sample of spectroscopically-pure germanium powder. The introduction of this impurity is undesirable because the ternary Fe-Ge-O system formed alters the stoichiometry of the alloy in an unpredictable way.

Attack of silica capsules by molten alloys was also observed, giving a brown reaction product in the region of contact. Chessin *et al.*¹³ note that SiO $_2$ is much more stable than GeO or GeO $_2$, and this is supported by the free energy changes of the following reactions:



estimated for a temperature of 1200°K from the thermodynamic data for oxides in Ref. 14. In the actual system, silica is present in the vitreous state, and reactants and products are not in standard states.

To examine the attack of silica by a 38 at. % alloy under controlled conditions, an experiment was carried out as follows: after degassing the alloy specimen in a silica crucible at about 10^{-5} torr and 600°C , the alloy was held molten at 1300°C for 4 h under 1 atm. of argon. Weight changes of both crucible and alloy were found to be less than 0.02 % after this treatment, and there

Table 2. Preparation and crystallisation of iron

Feedstock			Trans- port agent added as	Wt mg	Temp. in cryst. region °C	
At. % Ge	Phase analysis	Wt g				
(1)	50	FeGe ₂ + η^a	1.2	FeBr ₂	10	744
(2)	50	B35 FeGe ^a	0.95	I ₂	5	550
(3)	50	B35 FeGe ^b	6.55	I ₂	51	560
(4)	50	B35 FeGe ^c	6.5	I ₂	20	547
(5)	46	α + B35 ^b	0.15	FeBr ₂	2	742
(6)	50	B35 FeGe ^a	0.1	I ₂	~5	450
(7)	48	α + B35 ^a	0.27	FeBr ₂	8	720

^a powder.

^b lumps.

^c powder, with a few mg of the product from (2) added.

was no evidence under the microscope of attack on the silica. It can be concluded that a molten alloy will not attack silica if the system is properly outgassed, but that attack can sometimes occur in sealed evacuated capsules. In view of what has been said above on the oxygen content of alloys prepared by powder methods, it would seem to be unwise to melt such specimens in contact with silica, and in all cases alumina ware is to be preferred.

On the slow cooling of melts in the region of 50 at. % it is found that large crystals of primary β -phase formed at the bottom of the crucible and remained even after prolonged heating at lower temperatures. Rapid solidification is therefore necessary to give a fine primary structure that will react to give the low-temperature phases during a reasonably short period of heating.

Of the methods of preparing alloys described in Table 1, the second is probably the most satisfactory because of the smallness of the weight change and the improbability of contamination.

CHEMICAL TRANSPORT REACTIONS

Chemical transport with halogens or hydrogen halides is sometimes an extremely useful technique for growing crystals of compounds which decompose before the melting temperature is reached. The closely similar process of mineralisation is used when energy barriers to reaction, or a low rate of diffu-

germanides by mineralisation and transport.

Temp. differential °C	Vol. of capsule cm ³	Length of transport path cm	Duration of heating h	Wt transported mg	Products	Approx. crystal size cm
max. 1	~2	0	140	0	monoclinic FeGe	0.005
max. 1	~2	0	250	0	B20 FeGe	0.005
3	19	1.8	3000	1130	B35 FeGe	0.1 × 0.2
3	19	1.8	350	830	B20 FeGe	0.08
73	5	~8	300	83	monoclinic FeGe	0.005 × 0.02
50	~5	7	20	23	B20 FeGe	0.008
50	~4	~8	170	~10	α + B35 FeGe	0.005

sion lead to a slow reaction rate. Mineralisation is distinguished from transport by the fact that the latter process is then deliberately avoided by maintaining the reaction vessel at a uniform temperature. Material transport can then only take place between the grains of the specimen. For a more detailed account of the theory and applications of transport processes reference should be made to the recent monograph by Schäfer.¹⁵

Details of some mineralisation and transport experiments are given in Table 2. The mineralisation experiments (1) and (2) were used to prepare single-phase specimens of the high- and low-temperature polymorphs of FeGe, respectively. In the case of the high-temperature polymorph, the range of temperature within which this phase is stable is so small that the reaction $\eta + \text{FeGe}_2 \rightarrow \text{FeGe}_{(\text{monoclinic})}$ and the polymorphic transformation $\text{FeGe}_{(B35)} \rightarrow \text{FeGe}_{(\text{monoclinic})}$ are both rather slow at any temperature for which either of the reactions is possible. Under the catalytic influence of a trace of bromine either reaction goes to completion in a crushed (particle size about 1μ) specimen after heating for ten days or less. As pointed out in the following, the transformation $\text{FeGe}_{(B35)} \rightarrow \text{FeGe}_{(B20)}$ is so slow that it is unlikely that this phase can be prepared at all in a pure state without recourse to methods such as those discussed here. Two experiments were carried out to see if the polymorphic reaction could be hastened with the aid of a liquid menstruum of Cd or Bi. About 2 g of powdered B35 FeGe alloy and about 30 g of Cd or Bi was sealed in evacuated silica capsules and simultaneously heated and shaken

at 550°C for a period of about one week. Although the FeGe was wetted by the liquid in both cases, powder diffraction analysis of the residue after dissolving the solidified matrix did not show the presence of the low-temperature form of FeGe.

The transport experiments (5), (6), and (7) provided crystalline material for single-crystal X-ray studies, and experiments (3) and (4) are part of a current project to obtain large single crystals for the measurement of physical properties.

In experiments with bromine and iodine, it was found that the transport and mineralising effect of the latter decreased rapidly as the temperature was raised above about 600°C, whereas iodine was superior to bromine below this temperature. A mineralisation experiment exactly similar to (2) in all respects except for the substitution of FeBr₂ for I₂ gave a product which contained untransformed starting material.

The phases crystallising in a transport experiment were often found to vary from one experiment to another when attempts were made to repeat a particular crystallisation. The reason for this puzzling result was obscure until the following critical experiment showed that the growth was strongly influenced by alloy dust on the tube walls from the filling operation. A transport capsule similar to that of (4) was prepared, and heated at about 550°C for one day with the feedstock region of the tube at a temperature of about 540°C. After this period of 'back transport' the temperature relationships were changed so that the feedstock was at a higher temperature than the rest of the tube. No growth of crystals was observed until a temperature difference of 14°C was exceeded, and nucleation of seeds was rapid at a difference of 20°C. This is in direct contrast to the result of experiment (4) where crystal growth occurred with a difference of only about 3°C.

A tentative explanation can be put forward for the rather unexpected result of experiment (3), in which the B35 polymorph grew at a temperature below that of the transformation to the B20 form. Dust from the feedstock in this experiment would have been of the B35 form only, and the difference of 3°C is less than that required to exceed the critical supersaturation required for the nucleation of the stable phase. When the remaining feedstock was powdered, a few mg of B20 crystals added, and used as feedstock in (4) the crystals which grew were of the stable polymorph.

The main problem so far in attempts to grow large crystals has been that too many crystals grow, and tend to come into contact before they reach sizeable dimensions. The importance of removing active sites and the nuclei from feedstock dust is noted in a paper by Kaldis and Widmer.¹⁶

An experiment in progress suggests that a better control of nucleation can be achieved in a three-stage transport process. The first stage consists of a period of back-transport to destroy nuclei already present. A temperature difference is then applied and gradually increased until crystal growth can be observed with the aid of a telescope focussed on the tube. In the third stage, the temperature difference is decreased somewhat so that growth can take place without interference from further nucleation.

Fig. 1 shows the distribution of crystals in the tube at the end of experiment (5), and the temperature relationships during transport.

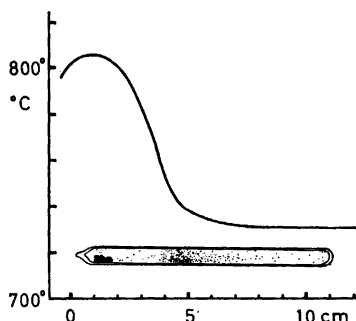


Fig. 1. The distribution of crystals in the tube at the conclusion of experiment 5 (see Table 2), and the temperature relationships during transport.

THERMODYNAMICS OF THE TRANSPORT PROCESS

Iodine transport of Ge occurs through the reaction:



(s = solid, g = gas) for which thermodynamic data are available.¹⁷ In the case of iron, the reactions:



and



are responsible for the vapor transport,¹⁸ with the former predominating at temperatures below about 700°C. Except at high temperatures and low pressures, the concentrations of I_2 and I in equilibrium with Ge are negligible.¹⁷

From these considerations it seems likely that the gas phase in equilibrium with FeGe under transport conditions will mainly consist of GeI_4 , FeI_2 , and GeI_2 , which are all sufficiently volatile at the experimental temperatures. The following reaction is proposed for the vapor transport of FeGe:



The observation that transport occurs from the feedstock to cooler regions implies that the transport reaction is endothermic.

From the following sources of enthalpy data:

	ΔH°_{298} for		Reference
	formation,	sublimation	
$\text{FeI}_{2(s)}$			19
$\text{I}_{2(s)}$		»	20
$\text{GeI}_{4(s)}$	»		21
$\text{GeI}_{4(s)}$		»	20
$2\text{GeI}_{2(s)} = \text{Ge}_{(s)} + \text{GeI}_{4(g)}$		disproportionation	12
$\text{GeI}_{2(s)}$	sublimation (estimated value)		12
$\text{FeSi}_{(s)}$	formation		20

the heats of reactions I—III below were estimated as follows:

		ΔH°_{298} (kcal/mole)
I	$\text{Fe}_{(s)} + \text{I}_{2(g)} = \text{FeI}_{2(g)}$	2
II	$\text{Ge}_{(s)} + 2\text{I}_{2(g)} = \text{GeI}_{4(g)}$	-40
III	$\text{Ge}_{(s)} + \text{GeI}_{4(g)} = 2\text{GeI}_{2(g)}$	30
IV	$\text{Fe}_{(s)} + \text{Ge}_{(s)} = \text{FeGe}_{(s)}$	x

and from these the value of ΔH°_{298} for reaction (4) was calculated to be $(68 - x)$ kcal/mole. Entropy data from the same sources lead to an estimated value of $(35 - y)$ e.u. for the value of ΔS°_{298} , where y is the entropy change of reaction IV.

The heat and entropy of formation of FeSi, which is isostructural with B20 FeGe, are -19 kcal/mole and 12 e.u., respectively, for standard states and 25°C . If the values for FeGe are of about the same order of magnitude, the entropy and enthalpy changes for eqn. (4) can be estimated to be ~ 20 e.u. and ~ 90 kcal/mole, respectively.

Transport reactions with a large positive enthalpy change must also have an entropy change of the same sign if significant transport effect is to be observed,¹⁵ and the proposed reaction complies with this principle.

CELL DIMENSIONS

Cell parameters are listed in Table 3. Standard deviations relate only to the self-consistency of the data, and do not include any estimate of systematic errors. As a consequence, variations in lattice parameters less than about 3σ are probably insignificant.

Cell dimensions of the η phase at the Ge-rich limit agree with values previously reported by Adelson and Austin,²² Kanematsu and Ohoyama,²³ and by Shtol'ts and Gel'd.¹¹ The values for B35 FeGe are also consistent with those measured by Kanematsu,²³ Ohoyama *et al.*,⁸ Nikolaev *et al.*,²⁴ Tomiyoshi *et al.*,²⁵ and by Shtol'ts and Gel'd,⁹ whilst the value of $a_0 = 4.9650 \pm 0.0005$ Å found by Adelson and Austin²² is at variance with the above determinations, although their value for c_0 is in good agreement. Values of the cell dimensions of FeGe₂ obtained in this investigation are also in agreement with the determinations of Shtol'ts and Gel'd,¹¹ Krén and Szabó,²⁶ and Yasukochi *et al.*²⁷

Attempts have been made to index the powder pattern of the α phase by analytical methods and from rotation and Weissenberg photographs of crystal-line material from halogen-transport preparations. Systematic twinning occurs in these crystals, and no reasonable interpretation of the symmetry has yet been obtained. Powder diffraction data is listed for this phase in Table 4 to aid in identification.

PHASE DIAGRAM

Phase relationships in the 38—72 at. % Ge region have been determined by the X-ray analysis of quenched alloys, and are shown in Fig. 2. Alloys with 38 at. % Ge were of the β phase only, and alloys with 40 at. % were single-phase η . The temperature of the polymorphic transformation B35 FeGe \rightarrow

Table 3. Cell dimensions of iron germanides in the region 42–72 at.% Ge.
 η -Phase (hexagonal indexing)

At.% Ge	Annealing temp. °C.	a Å	σa Å $\times 10^4$	c Å	σc Å $\times 10^4$
42	800	7.9805	4	4.9916	4
42	700	7.9804	4	4.9920	5
45	800	7.9817	18	4.9930	9

Monoclinic FeGe (CoGe-type)

At.% Ge	Anneal- ing temp. °C.	a Å	σa Å $\times 10^4$	b Å	σb Å $\times 10^4$	c Å	σc Å $\times 10^4$	β
50	740	11.838	10	3.9371	4	4.9336	4	103.514 \pm 0.007°
50 ^a	744	11.838	10	3.9359	3	4.9343	3	103.509 \pm 0.006°

^a the product from preparation (1), Table 2.

B35 FeGe (hexagonal indexing)

At.% Ge	Annealing temp. °C.	a Å	σa Å $\times 10^4$	c Å	σc Å $\times 10^4$
64	700°	5.0029	3	4.0551	3
47	720°	5.0027	3	4.0548	5

B20 (FeSi-type) FeGe

Prepared by	a Å	Experiment No. in Table 2.
iodine mineralisation at 550°C	4.700	(2)
bromine mineralisation at 550°C	4.701	
iodine transport at 450°C	4.698	(6)

Estimated standard deviation 0.002Å

C16 FeGe₂ (tetragonal indexing)

At.% Ge	Annealing temp. °C.	a Å	σa Å $\times 10^4$	c Å	σc Å $\times 10^4$
64	700	5.9074	6	4.9549	9
72	700	5.9072	5	4.9553	5

Ge in 72 at.% alloy annealed at 700° $a = 5.6579 \pm 0.0003$ Å.

monoclinic FeGe is so close to that at which α decomposes peritectoidally that the two temperatures could not be experimentally distinguished. The two reaction isotherms are shown slightly separated in the phase diagrams

Table 4. Powder diffraction pattern of single-phase α iron germanide prepared by iodine transport at 650°C from a feedstock with 42 at.% Ge. Taken in a Guinier-Hägg camera with strictly monochromatic $\text{CrK}\alpha_1$ radiation, and Si ($a = 5.4305 \text{ \AA}$) as internal standard.

$\sin^2\theta \times 10^5$	<i>I</i>	$\sin^2\theta \times 10^5$	<i>I</i>
2410	vvw	27753	m
10485	vvw	28498	w
10715	vvw	29118	vvw
10940	w	29175	w
12287	vvw	30114	m
14450	vvw	30200	st
15466	w	31108	w
17472	vvw	31189	m
18166	st	31691	st
18996	m	32220	st
19403	m	32740	vvw
19978	m	32833	vvw
20655	st	34103	st
21025	m	34292	vvw
21473	vvw	35230	vvw
21672	vw	38535	vvw
21806	vvw	38642	vvw
23148	vw	38744	vw
25695	vvw		

Lines marked vvw were very weak and the $\sin^2\theta$ values are approximate only.

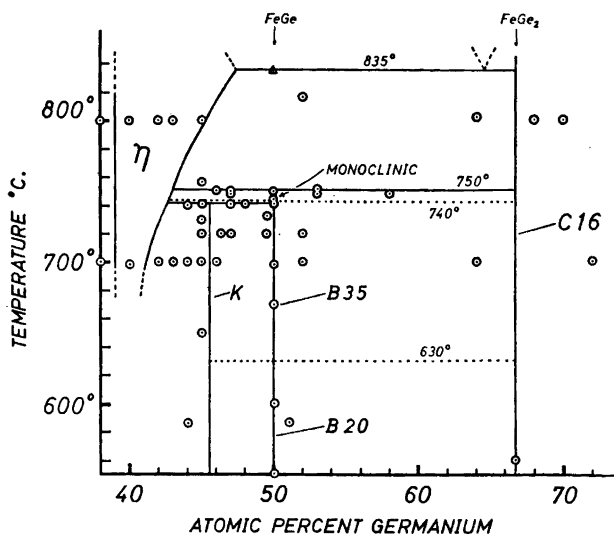


Fig. 2. Partial phase diagram for the Fe-Ge system in the region of 50 at.% Ge.

for the sake of clarity. Traces of B20 FeGe could be detected in a specimen of B35 FeGe that had been ground to a fine powder, pressed to a pastille, and heated at 580°C for several weeks. The accuracy of the transformation temperature shown on the phase diagrams is probably not better than $\pm 30^\circ\text{C}$. Other reaction temperatures determined in this investigation are considered accurate to about $\pm 2^\circ\text{C}$. It was found that the α phase became homogeneous at a composition between 45 and 46 at. % Ge.

Fig. 3 shows the partial diagram of the equiatomic region incorporated into a new phase diagram of the Fe-Ge system. Liquidus curves are adapted with minor changes from those determined by Ruttewit and Masing.² Phase boundaries of the lower part of the closed γ field were determined by Chessin *et al.*¹³ Lecocq and Michel²⁸ observed superstructure lines ($a' = 2a$) in alloys

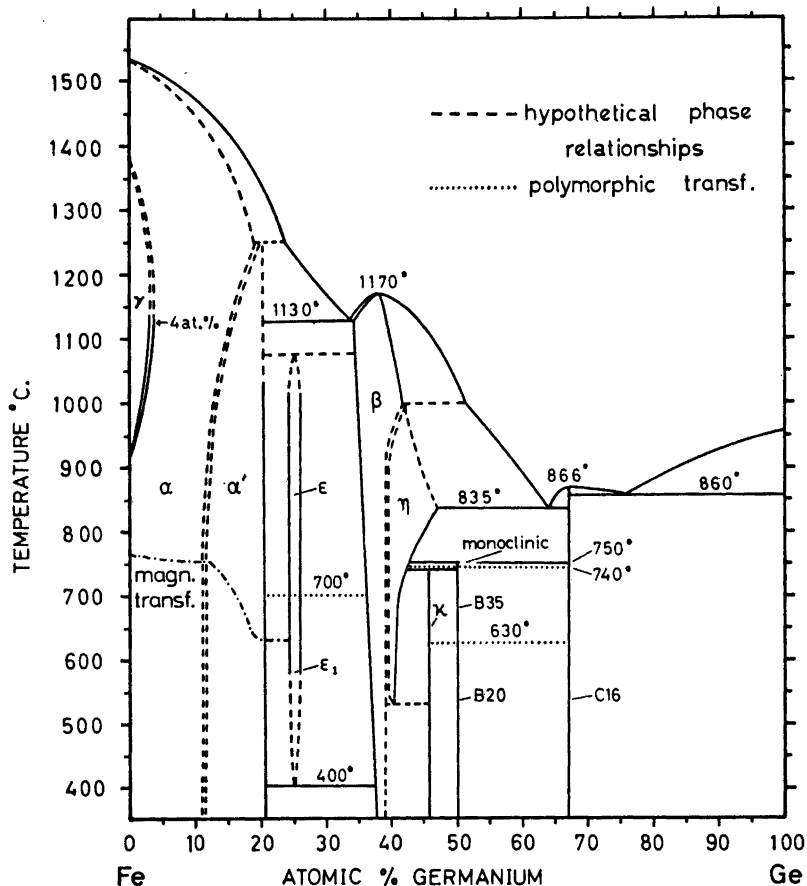


Fig. 3. Proposed phase diagram for the Fe-Ge system. Note added in proof: Recent work by prof. P. Lecocq (Faculté des Sciences, Orsay, France; private communication) will require a revision of the Fe-rich solid solution region of the phase diagram shown in Fig. 3.

between 13 and 18 at. % Ge, and also found that the ferromagnetic Curie temperature shows a steep decrease in this region (see Fig. 3). This is analogous to the case of Fe-Si alloys. Chessin *et al.*¹³ measured the change in the cubic cell dimension with Ge concentration, and found that this parameter remained constant for alloys with more than about 10.5 at. % Ge. They conclude that the Ge-rich boundary of the α solid solution is at this concentration, and evidently attribute the superstructure lines to the β phase. Kanematsu and Ohoyama²³ find that the Ge-rich boundary of the solid solution is at 20.4 at. % at 710°C. These authors also determined the temperature of the polymorphic transformation $\epsilon \rightarrow \epsilon_1$, and the composition limits of these Fe₃Ge phases. Adelson and Austin²² report that the microstructure of a 33 at. % alloy annealed at 1100°C showed eutectic regions of α -iron between the grains, and confirm the presence of this phase by X-ray methods. Kanematsu⁶ found a component with a Curie temperature of 825°K in a 33 at. % Ge specimen annealed at 1050°C, and concludes that this is α -iron. However, Kanematsu states that the α phase is metastable under these conditions, and that, furthermore, " ϵ and ϵ_1 never decompose to α and β phases".

On the other hand, Adelson and Austin²² find that *bcc* Fe is formed from ϵ_1 at 400°C, and it seems that further work is needed to clarify the phase relationships of Fe₃Ge. Partial diagrams for the β phase have been given by Adelson and Austin,²² Kanematsu,⁶ and by Shtol'ts *et al.*²⁹ All three diagrams agree quite well for the Fe-rich boundary, and this part of Fig. 3, together with the high-temperature region is taken from the diagram of Shtol'ts *et al.*²⁹ Kanematsu⁶ states that the ordered form of the β phase (*i.e.* η) is not a superstructure related to the latter by an order-disorder transformation, but a distinct phase. The Ge-rich region of the β field, together with the proposed decomposition of η by a eutectoid reaction at about 550°C is adapted from Kanematsu's phase diagram.

CONCLUSIONS

Recent studies of iron germanides have demonstrated the complexity of the Fe-Ge system. Chemical transport and mineralisation reactions have been found extremely useful in growing crystals at low temperatures, and to catalyse the change towards equilibrium at temperatures where annealing reactions are very slow. A study of the low-temperature phase relationships in this and other binary systems by means of these methods might bring to light many new phases for which the kinetic barriers to formation are otherwise too great. The observations on the preparation of alloys, together with the revised phase diagram, should be of considerable help in the future preparation of specimens for physical measurements. Further phase analytical work is indicated to settle some of the details of the equilibrium diagram.

Acknowledgements. I wish to thank Professor G. Hägg for the provision of laboratory facilities. For my introduction to this interesting field of research I am indebted to Dr. Allan Brown and Dr. Stig Rundqvist. I am also very grateful to Dr. Rundqvist for his interest in this work and for useful guidance.

The *Science Research Council* (London) is thanked for a research studentship. These investigations were financially supported by the *Swedish Natural Science Research Council* and by the *Fund for the Support of Younger Scientists* (Uppsala University).

REFERENCES

1. Richardson, M. W. *Acta Chem. Scand.* **21** (1967) 753.
2. Ruttevit, K. and Masing, G. *Z. Metallk.* **3** (1940) 52.
3. Castelliz, L. *Monatsh.* **84** (1953) 765.
4. Forsyth, J. B. and Brown, P. J. *Proceedings Intern. Conf. on Magnetism*, Nottingham 1964, Institute of Physics and the Physical Society, London 1965, p. 524.
5. Kanematsu, K. and Ohoyama, T. *Ibid.* p. 512.
6. Kanematsu, K. *J. Phys. Soc. Japan* **20** (1965) 36.
7. Olofsson, O. *Uppsala Univ. Private communication.*
8. Ohoyama, T., Kanematsu, K. and Yasukōchi, K. *J. Phys. Soc. Japan* **18** (1963) 589.
9. Shtol'ts, A. K. and Gel'd, P. V. *Russ. J. Phys. Chem.* **38** (1964) 1120.
10. Wallbaum, H. J. *Z. Metallk.* **35** (1943) 218.
11. Shtol'ts, A. K. and Gel'd, P. V. *Russ. J. Phys. Chem.* **36** (1962) 1301.
12. Jolly, W. L. and Latimer, W. M. *J. Am. Chem. Soc.* **74** (1952) 5757.
13. Chessin, H., Araj, S., Colvin, R. V. and Miller, D. S. *J. Phys. Chem. Solids* **24** (1963) 261.
14. Hodgman, C. D., (Ed.), *Handbook of Chemistry and Physics*, 43rd Ed., Chemical Rubber Publishing Co., Cleveland, Ohio 1961.
15. Schäfer, H. (Trans. Frankfort, H.), *Chemical Transport Reactions*, Academic, New York 1964.
16. Kaldis, E. and Widmer, R. *J. Phys. Chem. Solids* **26** (1965) 1967.
17. Jona, F., Lever, R. F. and Wendt, H. R. *J. Electrochem. Soc.* **3** (1964) 413.
18. Schäfer, H., Jacob, H. and Etsel, K. *Z. anorg. allgem. Chem.* **286** (1956) 42.
19. Brewer, L., Somayajulu, G. R. and Brackett, E. *Chem. Rev.* **63** (1963) 111.
20. Kubaschewski, O. and Evans, E. L. *Metallurgical Thermochemistry*, Pergamon, London 1958.
21. Evans, D. F. and Richards, R. E. *J. Chem. Soc.* **1952** 1292.
22. Adelson, E. and Austin, A. E. *J. Phys. Chem. Solids* **26** (1965) 1795.
23. Kanematsu, K. and Ohoyama, T. *J. Phys. Soc. Japan* **20** (1965) 236.
24. Nikolaev, V. I., Yakimov, S. S., Dubovtsev, I. A. and Gavrilova, Z. G. *J. E. T. P. Letters.* **2** (1965) 235.
25. Tomiyoshi, S., Yamamoto, H. and Wanatabe, H. *J. Phys. Soc. Japan* **21** (1966) 709.
26. Krén, E. and Szabó, P. *Phys. Letters* **11** (1964) 215.
27. Yasukōchi, K., Kanematsu, K. and Ohoyama, T. *J. Phys. Soc. Japan* **16** (1961) 429.
28. Lecocq, P. and Michel, A. *Bull. Soc. Chim. France* **5** (1962) 1412.
29. Shtol'ts, A. K., Gel'd, P. V. and Zagryazhskii, V. L. *Russ. J. Inorg. Chem.* **9** (1964) 76.

Received June 1, 1967.